Adaptive optimal operation of grid-connected battery systems under varying electricity market volatility

Citation for the original published paper (version of record):
Shabani, M. (2026). Adaptive optimal operation of grid-connected battery systems under varying electricity market
volatility. Energy Conversion and Management, 348.
http://dx.doi.org/10.1016/j.enconman.2025.120596

Energy Conversion and Management 348 (2026) 120596

Contents lists available at ScienceDirect

Energy Conversion and Management

journal homepage: www.elsevier.com/locate/enconman

Research Paper

Adaptive optimal operation of grid-connected battery systems under varying electricity market volatility

Masoume Shabani

Department of Electrical Engineering, Chalmers University of Technology, Gothenburg, Sweden

ARTICLE INFO

Keywords:
Battery energy storage systems
Electricity price volatility
Adaptive operation optimization
Grid-connected systems
Battery degradation
Charge-discharge scheduling

ABSTRACT

Battery energy storage systems are increasingly important for market-driven applications such as price arbitrage, yet their long-term profitability and durability depend strongly on how operations are scheduled. Conventional static or rule-based strategies often fall short of fully capturing opportunities in volatile electricity markets. This creates a need for adaptive approaches that respond optimally to electricity price variability while balancing short-term profitability with long-term battery health.

This study proposes a novel condition-responsive optimization strategy to evaluate how different levels of electricity market volatility affect optimal operational decisions, technical performance, and economic outcomes over the entire battery lifetime. The strategy dynamically adjusts daily charge–discharge frequency, duration, and timing in response to both market conditions and the internal state of the battery. The optimization objective is to identify an optimal trade-off between operational revenues and degradation-related costs, incorporating an advanced battery model that captures condition-dependent performance and degradation. To test adaptability, the strategy is applied to two contrasting market scenarios representing low and high price variability.

Results show that under the high-volatility scenario, the strategy increases annual profit by 80 % (€43,500 vs. €24,500 per installed MWh), raises net present value by 50 % (€415,500 vs. €279,000), and shortens payback time by 35 % (3.7 vs. 5.6 years) compared to the low-volatility case, while still maintaining nearly a decade of operation. These findings demonstrate that adaptive, market-aware scheduling significantly enhances profitability, favoring longevity-oriented operation in stable markets and revenue-driven cycling under volatile conditions.

The study provides practical insights into how dynamic, condition-responsive strategies perform under diverse market conditions, offering guidance for the development of more profitable, resilient, and sustainable energy storage systems.

1. Introduction

The transition toward more sustainable electricity systems is critical for meeting rising global electricity demand, achieving decarbonization goals, and mitigating the effects of climate change [1]. In response, power systems are undergoing a rapid transformation driven by the large-scale integration of variable renewable energy sources, particularly wind and solar. The recent International Renewable Energy Agency (IRENA) report highlights the rapid global deployment of wind and solar [2], while other studies emphasize the challenges of planning reliable systems based on these resources [3] and the implications of large-scale variable renewable integration [4]. However, this transition has introduced a range of challenges to the power system, including the intermittency of renewable generation [5], supply–demand imbalances [6,7], electricity price volatility [8], and the increasing need for flexible, fast-response resources to maintain grid stability and ensure market efficiency [9]. Grid-scale battery energy storage systems, based on the Lithium-ion (Li-ion) technology, have emerged as a promising solution to address these challenges. According to the International Energy Agency's Net Zero Scenario, global battery storage capacity is projected to expand 35-fold by 2030, reaching nearly 970 GW (GW), highlighting their pivotal role in future power systems [10,11]. Among their various applications, price arbitrage – the process of buying electricity at low prices and selling it at high prices – has garnered particular interest due to its potential for market-driven revenue generation [12,13]. The deployment of grid-scale battery storage for price arbitrage offers clear potential, yet its success depends on a combination of economic, technical, and operational factors. These aspects are examined in the following subsections. Section 1.1 summarizes key insights from prior studies on the economic viability of battery storage in price arbitrage. Section 1.2 provides an overview of scheduling approaches employed in existing works, with particular emphasis on their underlying assumptions and limitations. Section 1.3 discusses how battery degradation has been incorporated into prior research, and Section 1.4 outlines the broader limitations identified in prior studies. Building on these insights,

https://doi.org/10.1016/j.enconman.2025.120596
Received 8 June 2025; Received in revised form 7 September 2025; Accepted 28 September 2025
Available online 8 October 2025

Nomenclature

Abbreviations & Symbols

ICC_{batt}	Initial investment cost of battery system
BOL	Beginning of life
DOC	Depth of cycle
FEC	Full Equivalent cycle
LFP	Lithium iron phosphate
EOL	End of life
RTP	Real-time price
SOC	Battery state of charge
SOH	Battery state of health
opt	Optimal
C_{batt}	Battery capacity
C_{fade,cal_t}	Calendric capacity fade at time t (%)
C_{fade,cyc_t}	Cyclic capacity fade at time t (%)
C_{fade,tot_t}	Total capacity fade at time t (%)
$Cost_{deg,batt}$	Battery degradation cost (€)
$d_{ch\ (dch)}$	Charge/discharge duration (hours)
$I_{ch(dch),\ t}$	Battery charge (discharge) current at time t
$El_{w,t}$	Wholesale electricity price at time t
m	Number of days over project life;
n	Number of years over project life
NOC	Number of cycles per day
$P_{ch,t}$	Charge power at time t
$P_{dch,t}$	Discharge power at time t
PV	Present value
$R_{ch(dch),\ t}$	Battery internal resistance at time t
T	Temperature (K)
$time$	Passed time since the BOL (Sec)
t	Time step
$t_{ch,\ start,m}$	Start time indicator for charging the battery at day m
$t_{dch,\ start,m}$	Start time indicator for discharging the battery at day m
$V_{ch(dch),\ t}$	Battery terminal voltage during charging (discharging) at time t
X	Decision variable
$\alpha_{Replace}$	Battery replacement indicator

the main objectives and contributions of the present study are presented in Section 1.5.

1.1. Insights from prior studies on the economic viability of battery storage in price arbitrage

In market-based pricing structures, particularly day-ahead and real-time pricing (RTP) schemes, price signals fluctuate significantly on hourly and daily timescales [14,15]. This variability creates favorable conditions for battery energy storage systems to engage in price arbitrage by charging during low-price periods and discharging when prices are high to generate revenue [16]. A wide range of studies evaluated the economic potential of battery storage for price arbitrage across different regions and applications. Bradbury et al. [17] evaluated the internal rates of return (IRR) of 14 energy storage technologies for price arbitrage and reported negative IRR values for Li-ion batteries across seven U.S. electricity markets, indicating unprofitability under prevailing conditions. In the German market, Metz and Saraiva [18] analyzed intraday prices from 2011 to 2016 and, through sensitivity analysis, concluded that price volatility would need to increase roughly sevenfold for arbitrage to become profitable. Campana et al. [19] applied a Monte Carlo framework to assess Li-ion batteries for peak shaving, arbitrage, and photovoltaic self-consumption in commercial buildings in Johannesburg, Stockholm, and Rome, and found consistently negative net present values (NPV). Komorowska et al. [20] compared hydrogen storage and Li-ion batteries under two day-ahead scheduling scenarios, and found that although technically feasible, Li-ion systems remained economically unviable, with positive NPV achievable only if capital costs were reduced by about 75 %. Shcherbakova et al. [21] applied a Hotelling approach to South Korea's electricity market and showed that arbitrage revenues were insufficient to generate positive returns, while Lin and Wu [22] evaluated battery storage in the Chinese power market and similarly concluded that arbitrage was economically unviable under current cost structures. Peñaranda et al. [23] examined a grid-scale battery storage in the Colombian market and reported negative NPVs, reinforcing the limited viability of arbitrage in emerging economies.

Dufo-López [24] optimized the sizing and operation of grid-connected storage under real-time pricing conditions and demonstrated that arbitrage revenues remained insufficient to recover capital expenditures. Berg et al. [25] evaluated battery operation strategies in a Norwegian football stadium and showed that arbitrage revenues alone could not offset investment costs. Mustafa et al. [26] assessed a hospital-based storage system combining arbitrage with ancillary services and found negative NPVs when arbitrage was considered in isolation.

Núñez et al. [16] assessed arbitrage opportunities using 2019 data from several European day-ahead markets with a linear mixed-integer optimization model and reported consistently negative NPVs, with only modest differences across countries. More recently, Komorowska and Olczak [27] extended this analysis to 22 European markets using data from 2021 to 2022. Despite the increased price fluctuations, their results also showed negative NPVs under current Li-ion investment costs.

Collectively, these studies consistently demonstrate that, despite technical feasibility, battery storage for arbitrage has remained economically unattractive under current market conditions and capital cost structures across diverse geographies and applications. These consistent findings emphasize the need for more advanced operational strategies and cost reductions if battery storage is to become economically viable for arbitrage.

1.2. Scheduling approaches for battery price arbitrage

The way charging and discharging operations are scheduled to take advantage of electricity price differentials is a key factor influencing the profitability of battery storage applications. However, many previous studies on battery storage for price arbitrage have relied on static or rule-based scheduling strategies, which fail to fully exploit the opportunities presented by volatile electricity markets. A widely adopted approach is to predefine fixed peak and off-peak periods for operation, typically based on historical electricity price data. For example, Komorowska et al. [20], Komorowska and Olczak [27], Berg et al. [25], Mustafa et al. [26], and Dufo-López [24] all assumed that charging and discharging were scheduled at the same fixed times every day over extended periods, with only occasional adjustments across seasons or between weekdays and weekends [26]. While simple to implement, assuming fixed charging and discharging times may prevent the system from fully capturing profitable arbitrage opportunities in the volatile day-ahead electricity market, where the optimal price differentials may occur at times different from those initially planned.

To address this limitation, several studies explored more flexible strategies that adapt charge and discharge timings in response to dynamic electricity price conditions. For instance, Shcherbakova et al. [21] and Peñaranda et al. [23] assumed operation during the historical daily minimum and maximum prices, while Komorowska et al. [20] also investigated this type of scenario alongside a fixed scheduling approach. Although more responsive than purely static schedules, the effectiveness

of these methods may be limited under volatile real-time pricing conditions, where price trajectories can deviate substantially from historical patterns.

Other studies introduced more advanced techniques in their evaluations. For example, Telaretti et al. [28], and Shabani et al. [29] applied a moving-average filtering method to smooth price signals and determine optimal charge–discharge timings with the objective of maximizing daily profit under a specific dynamic price profile, while Telaretti et al. [30] employed an exhaustive search strategy by evaluating all possible combinations of daily maximum and minimum prices, selecting the pair with the widest gap to maximize daily revenue under a given price scenario. While these approaches enhanced scheduling flexibility and demonstrated revenue improvements compared to static strategies, these strategies failed to recover initial investment costs under the market conditions analyzed.

Another important limitation identified in prior studies is the assumption of fixed charge and discharge durations, represented by constant charge/discharge rate (C-rate). For example, Komorowska et al. [20], Dufo-López [24], and Telaretti et al. [28] all relied on constant charging and discharging rates in their analyses. Such assumptions limit the battery's flexibility to respond to sudden price spikes and capitalize on brief arbitrage windows [20]. Peñaranda et al. [23] demonstrated that increasing the C-rate enables faster charging and discharging, thereby allowing the battery to respond more effectively to rapid market fluctuations and to minimize exposure to less favorable periods. This highlights the importance of incorporating variable cycle durations into arbitrage strategies in order to enhance revenue capture under volatile market conditions.

In addition, most arbitrage strategies limit the battery system to a single cycle per day as assumed in prior studies [20,21,24–30]. However, allowing multiple cycles per day could increase the strategy's flexibility, enabling it to capture several significant price differentials within a single day [31].

Overall, reliance on static operational assumptions reduces the effectiveness of price arbitrage under dynamic pricing conditions and ultimately constrain potential revenue.

1.3. Consideration of battery degradation in arbitrage applications

Price arbitrage through battery storage introduces another layer of complexity—battery degradation [32,33]. Li-ion battery degradation is a complex process that occurs under all operating conditions, whether during storage (calendar aging) or during active use (cycling aging). However, batteries exhibit significantly different aging characteristics depending on the specific operating conditions and how they are used [34]. The degradation rate is significantly influenced by factors such as SOC, depth of cycle (DoD), C-rate, and temperature. More frequent or aggressive cycling may therefore increase revenue in the short term but accelerate degradation, leading to performance loss and higher replacement costs [35–39]. Despite its importance, many studies in this research area completely ignore degradation [16,17,20,21,26–30,40–44], while others consider it only after the optimization process [24,45–48]. Even when degradation is included, it is often modeled using overly simplified assumptions that neglect the dynamic and condition-dependent nature of battery degradation, thereby failing to integrate its effects into operational decision-making. Such simplifications overlook the strong interdependence between control strategies and degradation progression. As a result, arbitrage strategies that neglect degradation dynamics under variable operating conditions may overestimate profitability and misrepresent long-term economic viability.

1.4. Limitations of prior studies and research gap

In summary, the success of battery storage arbitrage in dynamic electricity markets critically depends on multiple operational factors, including cycle frequency, charge/discharge timing, and cycle duration, all of which influence both revenue generation and battery degradation. Although a wide range of approaches have been applied to price arbitrage strategies, as highlighted in Section 1.2, many existing studies rely on simplifying assumptions that limit their applicability under volatile market conditions.

A central limitation is the widespread use of static or rule-based scheduling strategies, which assume fixed operational parameters such as predefined charging and discharging times, constant charge/discharge durations, and restricting operation to a single cycle per day. Importantly, most arbitrage strategies fail to optimize all these factors holistically, overlooking their interconnected effects and thereby constraining battery utilization and limiting potential revenue.

Battery degradation introduces an additional challenge. As noted in Section 1.3, while some works include degradation effects, many either neglect them altogether or evaluate degradation only after scheduling decisions are made. Even when considered, degradation is often modeled with oversimplified assumptions that fail to capture its nonlinear and condition-dependent nature. This limits the integration of degradation costs into arbitrage decision-making and risks overestimating long-term profitability.

Overall, the literature reveals a lack of advanced adaptive scheduling strategies that can dynamically align battery-level operational decisions with system-level performance objectives while responding optimally to both volatile electricity price signals and condition-dependent battery degradation. Such strategies are essential for achieving short-term profitability and long-term operational sustainability. Moreover, the performance of such condition-responsive scheduling strategies under varying levels of market volatility remains largely unexplored, leaving a critical gap in understanding how electricity price dynamics shape optimal operational decisions and influence the long-term technical and economic outcomes of battery storage systems.

1.5. Main contributions and objectives of the present study

To address the research gap identified in prior studies (Section 1.4), the main objectives and contributions of this study are summarized as follows:

- For the first time, this study systematically analyzes how electricity market volatility influences optimal operational decisions across battery lifetime, as well as long-term economic outcomes under an advanced condition-responsive scheduling strategy. Two distinct market scenarios are considered: one characterized by high price volatility and another by low volatility.
- A novel condition-responsive optimization strategy is developed to schedule battery usage in response to both electricity market signals and internal battery dynamics. It jointly optimizes three cycle characteristics—(a) frequency, (b) timing, and (c) duration. By leveraging day-ahead electricity prices and battery state information, the framework dynamically adjusts these parameters to maximize daily revenue while minimizing degradation-related costs. This approach effectively links battery-level operating decisions with system-level performance objectives, promoting both profitability and battery longevity.
- The study comprehensively evaluates the optimized daily operational scheduling decisions (a–c) across the entire battery lifetime, alongside key techno-economic performance indicators such as annual profit per installed MWh, battery lifetime, total revenue, NPV, return on investment (ROI), and payback period.

Overall, this study provides a deeper understanding of how dynamic, condition-responsive battery management strategies perform under different market conditions, offering insights that can inform the design of more profitable, resilient, and sustainable energy storage systems.

2. Method

This section outlines the methods employed in this study. Section 2.1 presents the developed multi-aspect battery modeling framework. Section 2.2 introduces the proposed adaptive operation optimization strategy, including the optimization objectives, decision variables, and procedures. Section 2.3 describes the operational strategy implemented for grid-connected battery systems. Finally, Section 2.4 explains the metrics used to assess the system's economic viability.

2.1. Multi-aspect battery modeling framework

This work adopts a comprehensive battery modeling framework designed to capture Li-ion battery behavior under varying operational conditions. Key parameters assessed include terminal voltage, calendar and cycle-induced capacity fade, state-of-health (SOH), SOC, and battery lifetime. The methodology and governing equations for these metrics are described in the following subsections, with detailed formulations presented in Appendix A. This study focuses on a lithium iron phosphate (LFP) battery, selected for its suitability in grid-scale energy storage applications due to its affordability, inherent safety, high energy density, long service life, and use of environmentally benign materials [50,51]. A summary of the selected battery's specifications is provided in Table B1 (Appendix B).

2.1.1. Battery electrical performance and aging modeling

To simulate the current–voltage (I–V) characteristics of the battery, this study employs an equivalent circuit-based electrical model. The model consists of an internal resistance element (R) and an open-circuit voltage (OCV) source, both of which vary as function of the battery's operational state and which are based on experimental data. This approach strikes a balance between computational simplicity and predictive accuracy [52], making it suitable for stationary applications. The full expressions for terminal voltage under charging and discharging conditions are provided in Appendix A (Eqs. A(1)–A(2).

To accurately predict capacity degradation and battery lifetime under varying operational conditions, such as DOC, C-rate, SOC, cycle frequency, and temperature, this study incorporates a detailed cyclic and calendric degradation model developed by Naumann et al. [36,38]. The model accounts for the major aging-influencing factors under real operational scenarios, including SOC, DOC, elapsed time since beginning-of-life (BOL), full equivalent cycles (FEC), and charge/discharge C-rates, and ambient temperature (fixed at 25 °C; typical for stationary applications [35,38]). Total capacity fade is calculated by superimposing calendar and cyclic aging effects. The corresponding formulations are provided in Appendix A (Eqs. A(3)–A(6), and Table A1). The predictive accuracy of this model has been validated in literature [36,38] through comprehensive studies under dynamic stress profiles, demonstrating its ability to precisely estimate capacity loss over extended periods and varying load conditions.

To identify stress factors contributing to battery degradation, this study implements a half-cycle (event-based) counting approach. Transitions between charging and discharging are detected by changes in the sign of battery power or the SOC gradient [38]. After each half-cycle, parameters including DOC, charge/discharge C-rate, and average SOC are captured and used as inputs to the cyclic aging model. By accurately capturing partial cycles and stress variations, this approach enables more precise aging estimation under realistic, time-varying conditions.

2.1.2. Battery state-of-health, state-of-charge, and lifetime

- *Battery state-of-health (SOH)*: the SOH reflects the extent of battery degradation by measuring the ratio of the current capacity to the original capacity [35], as formulated in Eq. (1). SOH is a vital metric for determining battery performance, managing operation, and planning replacements. In this study, SOH is continuously monitored and predicted under real operating conditions as part of the system's management and optimization strategy.

$$SOH_t = \frac{C_{\text{batt}_t}}{C_{\text{batt, BOL}}} \times 100 = \frac{C_{\text{batt,BOL}} - C_{\text{fade, tot}_t}}{C_{\text{batt, BOL}}} \times 100 \quad (1)$$

- *Battery state-of-charge (SOC)*: The SOC of a battery represents the current energy level relative to its full capacity [53]. In this study, SOC is estimated at each time step t using the Coulomb counting method, as shown in Eq. (2). The Coulomb counting method is widely used for SOC estimation, as it tracks the amount of charge flowing in and out of the battery over time [53]. To account for capacity fade, SOC is calculated relative to the actual capacity at time t (i.e., $SOH_t \times C_{\text{batt, BOL}}$), as reflected in Eq. (2). In this study, the SOC operation window is constrained between the lower and upper admissible limits of SOC, as formulated in Eq. (2) and further detailed in Section 2.2.3.

$$SOC_{t+1} = SOC_t - S_{\text{ch}} \frac{\int I_{\text{ch},t}\,dt}{SOH_t \times C_{\text{batt, BOL}}} + S_{\text{dch}} \frac{\int I_{\text{dch},t}\,dt}{SOH_t \times C_{\text{batt, BOL}}} \quad (2)$$

$$SOC_{Min} \le SOC_t \le SOC_{Max}, \forall t$$

To prevent simultaneous charging and discharging, a constraint is applied such that $(S_{\text{ch}} + S_{\text{dch}}) \le 1$. Here, S_{ch} and S_{dch} are binary decision variables indicating charging mode and discharging mode, respectively. When the battery is in idle mode, both variables are zero. $I_{\text{ch},t}$ and $I_{\text{dch},t}$ denote the charging and discharging currents at each time step t, respectively. By convention, a negative current ($I_{\text{ch},t} < 0$) indicates charging mode, whereas a positive current represents discharging. SOH_t is the battery state of heath at each time t, and $C_{\text{batt, BOL}}$ is the rated battery capacity at the BOL.

- *Battery lifetime:* The total battery lifetime is not pre-assumed in this study. Instead, it is defined as the time span from the BOL until the point when SOH falls below a specified end-of-life (EOL) threshold, as shown in Eq. (3). For this analysis, a threshold SOH of 75 % is used to define the EOL, consistent with typical warranty specifications for LFP batteries in stationary applications.

$$LF_{\text{batt}}(\text{yr}) = \frac{\sum t_{(SOH \le \alpha_{\text{Replace}})}}{8760} \quad (3)$$

2.2. Adaptive operation optimization strategy in response to market dynamics and battery behavior

This section presents the proposed adaptive operation optimization strategy, designed to manage battery usage in response to both electricity market fluctuations and the internal battery performance dynamics. Leveraging day-ahead electricity price and real-time battery state information, the optimization framework dynamically adjusts cycle characteristics on a daily basis to maximize revenue while minimizing degradation-related costs, thereby ensuring long-term performance and reliability. Key optimization variables include the number of charge–discharge cycles per day, the start times for charging and discharging, and the duration and power rate of each cycle. This approach establishes a strong connection between battery-level operating decisions and system-level performance objectives, supporting both profitability and battery longevity. Fig. 1 provides an overview of the overall optimization framework, illustrating how the decision-making phase (scheduling) and the operation phase (execution) interact to achieve the defined operational objectives.

In brief, given the day-ahead electricity market profile, the decision-making phase determines an optimized charging and discharging plan for the upcoming day to ensure effective battery utilization. These

optimized schedules are then passed to the operation module, which controls the battery accordingly.

The mathematical definitions of the objective functions and decision variables are provided in Subsections 2.2.1–2.2.2, followed by a description of the state variables and operational constraints in Subsections 2.2.3–2.2.4. The complete optimization workflow is detailed in Subsection 2.2.5.

2.2.1. Formulation of optimization objectives

As formalized in Eq. (4), the objective of the proposed optimization framework is to maximize daily operational revenue while minimizing battery degradation-related costs. These two objectives are optimized concurrently to determine the system's optimal daily profit, as defined in Eq. (5). These objective functions are driven by a set of decision variables introduced in the following subsection. The formulations used to compute daily revenue and degradation cost are available in Appendix C (Eqs. C1 and C2).

$$\begin{cases} \text{Maximize}: Revenue_m\left(X_{1,m}, X_{2,m}^{(z)}, X_{3,m}^{(z)}, X_{4,m}^{(z)}, X_{5,m}^{(z)}\right) \\ \text{Minimize}: Cost_{\text{deg,batt}_m}\left(X_{1,m}, X_{2,m}^{(z)}, X_{3,m}^{(z)}, X_{4,m}^{(z)}, X_{5,m}^{(z)}\right) \end{cases} \rightarrow \text{maximize} Profit_m; m = 1, \cdots, \text{days till EOL} \tag{4}$$

- $X_{3,m}^{(z)}$: discharging duration for each cycle
- $X_{4,m}^{(z)}$: start time of charging for each cycle
- $X_{5,m}^{(z)}$: start time of discharging for each cycle

Here, the subscript m denotes the operational day, and the superscript (z) indexes the cycle within that day:

- z = 0: full-day cycle (single cycle per 24 h),
- z = 1: first half of day (00:00–12:00),
- z = 2:: second half of day (12:00–24:00).

For z = 0, the system operates under a single-cycle configuration, permitting at most one complete charge–discharge cycle within a 24-hour horizon. In this scenario, five decision variables must be specified for each day m: $\left(X_{1,m}, X_{2,m}^{(0)}, X_{3,m}^{(0)}, X_{4,m}^{(0)}, X_{5,m}^{(0)}\right)$ as detailed in Eqs. (6) – (10).

When $z = 1$ or $z = 2$, the algorithm supports semi-daily cycling, enabling up to two complete cycles within the same 24-hour horizon. In this case, the day is divided into two equal time blocks: the first period ($z = 1$) spans from 00:00 to 12:00, and the second period ($z = 2$) spans from 12:00 to 24:00.

Under this setting, a total of nine decision variables must be determined for day m: four for the first half of the day $\left(X_{2,m}^{(1)}, X_{3,m}^{(1)}, X_{4,m}^{(1)}, X_{5,m}^{(1)}\right)$, and four for the second half $\left(X_{2,m}^{(2)}, X_{3,m}^{(2)}, X_{4,m}^{(2)}, X_{5,m}^{(2)}\right)$. If the optimization determines that cycling is not economically beneficial on a given day, the system remains in idle mode, represented by $NOC_m = 0$, and no operational decision variables are applied. Additional implementation details can be found in Section 2.3.5.

$$Profit_{\text{opt},m}\left(X_{1,\text{opt},m}, X_{2,\text{opt},m}, X_{3,\text{opt},m}, X_{4,\text{opt},m}, X_{5,\text{opt},m}\right) = MAX\left(Revenue_m\left(X_{1,m}, X_{2,m}^{(z)}, X_{3,m}^{(z)}, X_{4,m}^{(z)}, X_{5,m}^{(z)}\right) - Cost_{\text{deg,batt}_m}\left(X_{1,m}, X_{2,m}^{(z)}, X_{3,m}^{(z)}, X_{4,m}^{(z)}, X_{5,m}^{(z)}\right)\right) \tag{5}$$

2.2.2. Definition of decision variables

The decision variables used in this optimization problem are defined in Eq. (6)– (10).

$$\begin{cases} X_{1,m} = NOC_m; z = \begin{cases} 0, NOC_m = 1 (\text{daily-periodicity}) \\ 1, 2 NOC_m = 2 (\text{semi-daily periodicity}) \end{cases} \\ X_{2,m}^{(z)} = d_{\text{ch},m}^{(z)} = \begin{cases} d_{\text{ch},m}^{(0)}; & z = 0 \\ (d_{\text{ch},m}^{(1)}, d_{\text{ch},m}^{(2)}); & z = 1, 2 \end{cases} \\ X_{3,m}^{(z)} = d_{\text{dch},m}^{(z)} = \begin{cases} d_{dch,m}^{(0)}; & z = 0 \\ (d_{\text{dch},m}^{(1)}, d_{\text{dch},m}^{(2)}); & z = 1, 2 \end{cases} \\ X_{4,m}^{(z)} = t_{\text{ch, start},m}\left(X_{2,m}^{(z)}, RTP_m\right) = \begin{cases} t_{\text{ch,start},m}^{(0)}; & z = 0 \\ (t_{\text{ch,start},m}^{(1)}, t_{\text{ch,start},m}^{(2)}); & z = 1, 2 \end{cases} \\ X_{5,m}^{(z)} = t_{\text{dch, start},m}\left(X_{3,m}, RTP_m\right) = \begin{cases} t_{dch,start,m}^{(0)}; & z = 0 \\ (t_{\text{dch,start},m}^{(1)}, t_{\text{dch,start},m}^{(2)}); & z = 1, 2 \end{cases} \end{cases} \tag{6-10}$$

Here, the decision variables are defined as follows:

- $X_{1,m}$: number of charge–discharge cycles per day
- $X_{2,m}^{(z)}$: charging duration for each cycle

2.2.3. Operational constraints and feasibility conditions

To maintain safe and efficient battery operation, the model incorporates a set of system-level constraints. These include limits on cycle frequency, SOC operation window, charge/discharge power, and EOL conditions.

The number of charge–discharge cycles per day is restricted to a maximum of two (NOCm $\leq$ 2), balancing technical and market-driven considerations. Most wholesale electricity markets exhibit two price peaks per day, and additional cycling can accelerate degradation and reduce battery efficiency. This constraint ensures alignment with market opportunities while preserving long-term battery health. To prevent harmful overcharging and deep discharging, the SOC operation window is constrained within the range of 10 % to 95 %.

The battery is considered to reach its EOL when its SOH declines to 75 %, corresponding to the replacement threshold $\delta_{\text{replace}} = 75$ %. This criterion is consistent with typical manufacturer warranties for LFP batteries and ensures timely replacement before significant performance loss.

The charge and discharge power limits are dynamically calculated based on the battery's available capacity and the maximum allowable C-rates. Instead of being fixed, the charge and discharge C-rates are implicitly adjusted through the optimization of charge and discharge durations.

It is worth mentioning that this study assumes unrestricted interaction with the grid at the battery's rated power. In practice, distribution

networks may impose limits on power injection or absorption due to grid capacity, congestion, or stability considerations. Under such conditions, the framework would still operate within the admissible range, maintaining the same optimization logic but with reduced maximum power throughput, which could lower revenues, particularly in high-volatility markets where sharp, short-term price spikes provide valuable arbitrage opportunities. Maintaining similar profitability under strict grid limits may require larger battery sizing.

2.2.4. State variables for optimization

Eq. (11) defines the battery state variables, which are monitored and updated on an hourly basis, then passed to the decision-making module at the end of each day to support the next optimization step.

At the beginning of the first day (m = 1), the battery is assumed to be unused, and the initial SOC is set to its maximum level. For all subsequent days (m ≠ 1), the initial values of SOC, SOH, and remaining capacity are carried over from the final recorded state of the previous day (i.e., the last hourly update of day m − 1).

2.2.5. Optimization algorithm

In response to the day-ahead electricity price profile, the proposed optimization algorithm determines the most profitable battery operation plan for each day by systematically exploring all feasible combinations of decision variables within the defined search space. The full algorithm is outlined below:

The process begins by initializing the battery's state variables—SOC, capacity, and SOH—as defined in Equation (16). At the start of each day m, the decision-making module receives the 24-hour ahead electricity price data, which serves as the basis for optimization. The algorithm examines both single-cycle ($z = 0$) and dual-cycle ($z = 1, 2$) configurations by setting the number of daily charge–discharge cycles to either one or two. If the algorithm determines that cycling is not economically viable, the battery remains in idle mode ($NOCm = 0$). For each potential cycle configuration, charging and discharging durations are initialized within practical operational limits: 1–10 h for full-day cycles and 1–6 h for semi-daily cycles. Given every combination of charge/discharge duration, the algorithm identifies the optimal start times that maximize daily price differentials. Then, for each unique combination of

$$\begin{cases} U_m^1 = SOC_{\text{initial},m} = \begin{cases} SOC_{\text{final},m-1}\left(X_{1,\text{opt},m}, X^{(z)}_{2,\text{opt},m}, X^{(z)}_{3,\text{opt},m}, X^{(z)}_{4,\text{opt},m}, X^{(z)}_{5,\text{opt},m}\right); m \neq 1 \\ SOC_{\text{Min}}\ ; m = 1 \end{cases} \\ U_m^2 = SOH_{\text{initial},m} = \begin{cases} SOH_{\text{final},m-1}\left(X_{1,\text{opt},m}, X^{(z)}_{2,\text{opt},m}, X^{(z)}_{3,\text{opt},m}, X^{(z)}_{4,\text{opt},m}, X^{(z)}_{5,\text{opt},m}\right); m \neq 1 \\ SOH_{\text{BOL}}\ ; m = 1 \end{cases} \\ U_m^2 = C_{\text{bat initial},m} = \begin{cases} C_{\text{bat final},m-1}\left(X_{1,\text{opt},m}, X^{(z)}_{2,\text{opt},m}, X^{(z)}_{3,\text{opt},m}, X^{(z)}_{4,\text{opt},m}, X^{(z)}_{5,\text{opt},m}\right); m \neq 1 \\ C_{\text{bat BOL}}\ ; m = 1 \end{cases} \end{cases} \tag{11}$$

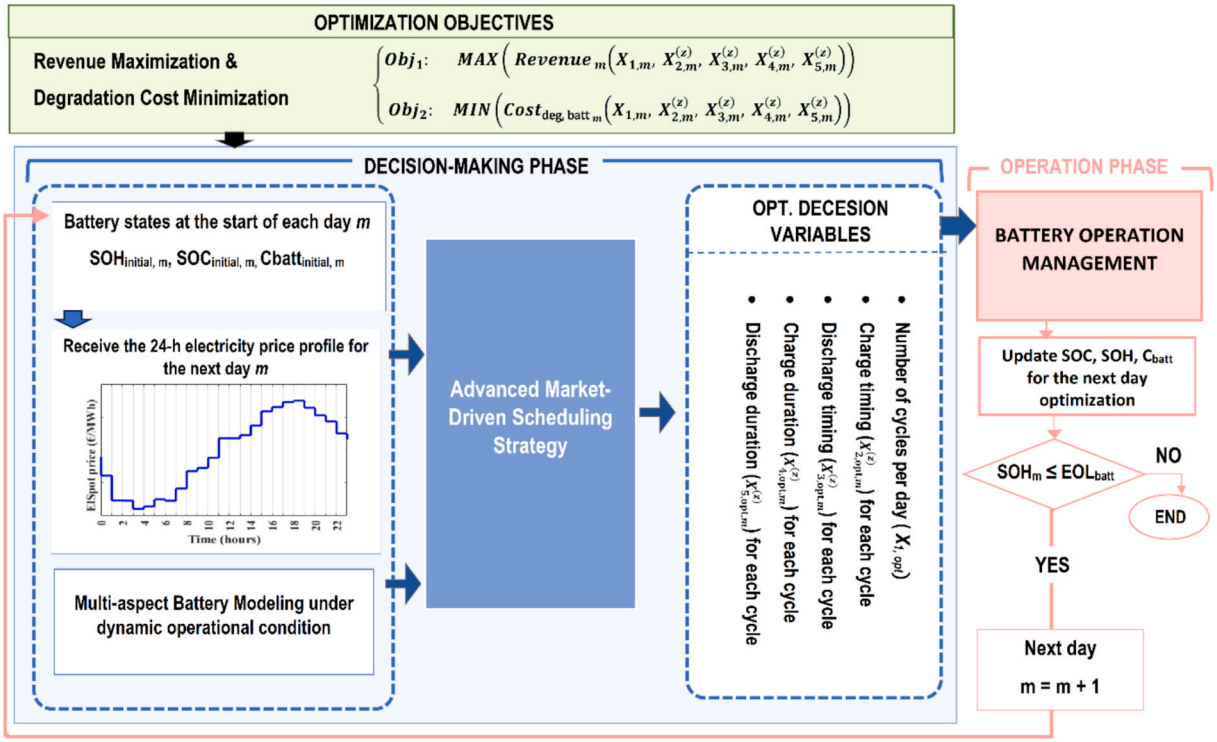

Fig. 1. Overview of the proposed adaptive, market-driven operation optimization strategy.

aforementioned decision variables, the objective functions—which maximize revenue while minimizing degradation cost—is evaluated following the operational strategy described in Section 2.4. Results from all configurations are stored in a central database. After evaluating all feasible options, the configuration that yields the maximum daily profit is selected as the optimal schedule for day m. After iterating through all feasible decision variable combinations, the configuration that yields the highest profit is selected as the optimal schedule for day m. The selected schedule, consisting of the variables $X_{1,\mathrm{opt},m}$, $X_{2,\mathrm{opt},m}$, $X_{3,\mathrm{opt},m}$, $X_{4,\mathrm{opt},m}$,$X_{5,\mathrm{opt},m}$, is passed to the battery operation module. This module implements the schedule, updates the battery state variables accordingly, and feeds the updated state back into the optimization loop to initialize day m + 1. This daily optimization loop continues until the battery's SOH reaches its defined end-of-life threshold, allowing the strategy to adapt to a wide range of market conditions and evolving battery behavior. At the end of the simulation, the model outputs a set of optimized operational strategies, along with the corresponding techno-economic performance metrics and the battery degradation trajectory over the battery lifetime, which will be detailed in Section 2.4.

2.3. Operational strategy of grid-connected battery system

The operational strategy developed in this study is designed to simulate the hourly performance of a grid-connected battery system over its life period. Its core objective is to take advantage of fluctuations in electricity market prices to maximize revenue. The strategy enables continuous monitoring and adaptive control of battery behavior throughout its lifetime charging and discharging actions are carried out according to optimized schedules generated by the adaptive operation optimization strategy (see Section 2.3). At the beginning of each day, the strategy receives the following input:

- The 24-hour day-ahead market clearing price profile. The focus of this study is on day-ahead prices, which are fully published in advance by the market operator (see Section 3) for the following day. Since these prices are officially cleared and represent the actual information available to market participants prior to operation, they provide a reliable and accurate input for forward-looking scheduling decisions. The distinction between day-ahead and real-time markets has been widely discussed in recent studies [54,55], which highlight the strong correlation between them.
- Initial values of battery SOC, SOH, and capacity
- Operational constraints (e.g., maximum allowable charging/discharging power, SOC limits, and SOH threshold)
- The optimized operation schedule for that day, including cycle frequency, start times, and charge/discharge durations, which were optimized in response to market signals and the internal battery dynamics.

Based on these inputs, the system charges the battery during the optimized charging window ($t_{ch,start,m} \le t_m \le t_{ch,start,m} + d_{ch}$), at the maximum allowed charging rate ($P^{\mathrm{ch}}_{\mathrm{min,t}}$) using low-cost grid electricity. Discharging occurs within the optimized discharge window ($t_{dch,start,m} \le t_m \le t_{dch,start,m} + d_{dch}$) also at the maximum permissible rate ($P^{\mathrm{ch}}_{\mathrm{max,t}}$). During all other hours, the battery remains in an idle state. At each time intervals, the following steps are carried out:

- Update SOC based on current input/output flow (Eq. 8)
- Estimate degradation by applying calendric and cyclic aging models (Section 2.2)
- Update SOH according to the battery's remaining capacity (Eq. (4)

This loop is repeated continuously throughout the day. At day's end, the updated battery state variables — SOC, SOH, and capacity — are passed to the decision-making module to inform the scheduling of operations for the following day. The process continues daily until the battery reaches its EOL threshold (e.g., SOH $\le$ 75 %), enabling long-term, behavior-aware operation under dynamic market conditions.

Table 1
Optimal technical and economic results derived from system optimization for a 1 MWh battery system under Scenarios 1, and 2.

	Scenario 1	Scenario 2
PPEI (€/MWh/year)	24,500	43,500
NPV (€)	279,000	415,500
ROI (%)	79.7	118.7
Lifetime (year)	11.3	9.6
PBP (year)	5.6	3.7

Table 2
Financial performance metrics and their formulations.

Metric	Equation	
Net present value (NPV)	$\mathrm{NPV} = \sum_{n=1}^{LF_{\mathrm{batt}}(\mathrm{yr})} \frac{\mathrm{Revenue}_{\mathrm{opt},n}}{(1+\mathrm{r})^n} - ICC_{\mathrm{batt}}$	(12)
Return on Investment (ROI)	$\mathrm{ROI}\ (\%) = \frac{\mathrm{NPV}}{ICC_{\mathrm{batt}}} \times 100$	(13)
Payback period (PBP)	$\mathrm{PBP}\ (\mathrm{yr}) = \frac{m(\sum_m Revenue_{\mathrm{opt},m} - ICC_{\mathrm{batt}}) \ge 0)}{365}$	(14)
Annual Average Profit Per Unit of Energy Installed (PPEI)	$\mathrm{PPEI}\ (€/\mathrm{kWh/yr}) = \frac{\mathrm{NPV}}{C_{\mathrm{batt,\,BOL}} \times LF}$	(15)

2.4. Economic viability assessment metrics

To evaluate and compare the economic viability of the battery system under different market and operational scenarios, four key financial metrics are employed. Table 2 summarizes each metric, and the corresponding mathematical formulation.

NPV represents the cumulative profit generated by the project over its lifetime. As indicated in Eq. (12), it is calculated as the sum of the annual revenue contributions for each year n, discounted to their present value using a discount rate, minus the initial capital cost of the battery.

ROI is a key metric for assessing the potential profitability of capital projects. As shown in Eq. (13), it is calculated as the ratio of NPV to the initial investment cost of the battery.

PBP is a financial indicator that estimates how long it will take for an investment to generate positive cash flow and recover the initial investment cost, as formulated in Eq. (14).

Annual Average *PPEI* quantifies the profitability of a battery storage system relative to its installed energy capacity. This metric is particularly useful for comparing different projects or configurations. As defined in Eq. (15), it is computed by dividing the present value of total profit by the product of two factors: the battery's rated energy capacity and its operational lifetime.

3. Case study overview: Market variability scenarios

This study optimizes battery cycle characteristics over an extended period under two distinct electricity market scenarios to evaluate how varying market dynamics impact optimal operational strategies, technical performance and economic outcomes. Scenario 1 represents a market with relatively lower price variability, whereas Scenario 2 reflects a high-volatility electricity market. The scenarios were selected based on distinct statistical characteristics, ensuring broad applicability to various electricity markets. The electricity market data were sourced from the European Network of Transmission System Operators for Electricity (ENTSO-E) Transparency Platform [56], covering hourly day-ahead Elspot prices for the year 2022. Scenario 1 corresponds to the Swedish SE3 bidding zone, while Scenario 2 corresponds to the Romanian bidding zone. These two zones were selected to represent

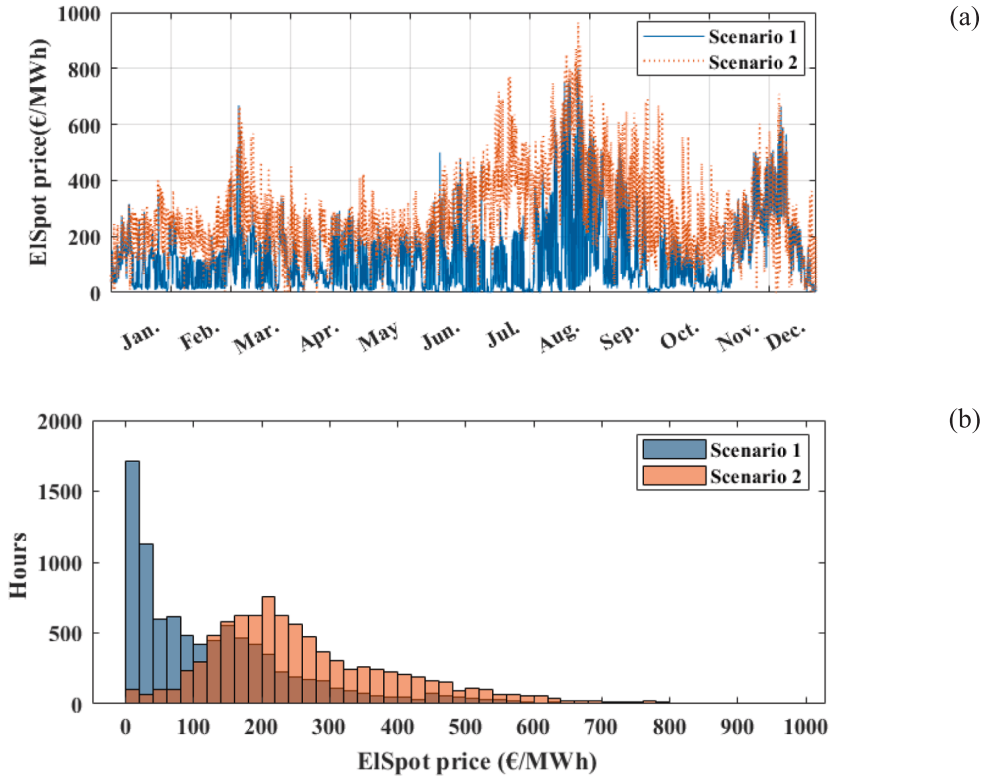

Fig. 2. (a) Hourly price profiles and (b) price distribution histograms for Scenario 1 (low variability, Sweden SE3) and Scenario 2 (high variability, Romania), based on day-ahead Elspot prices [56].

contrasting market conditions within Europe, thus providing a suitable basis for evaluating the adaptability of the proposed optimization strategy under both low- and high-volatility conditions. Further details and statistical characteristics of each scenario are presented in Subsections 3.1 and 3.2. It is worth noting that the optimization strategy developed in this study remains applicable to any electricity pricing environment, independent of specific market conditions.

Fig. 2 illustrates the hourly price profiles over a full year for both scenarios, along with histograms of price distributions, highlighting the extent of price fluctuations.

3.1. Scenario 1: Low electricity price variability

Scenario 1 corresponds to the Swedish SE3 bidding zone, which is part of the Nordic electricity market. Prices in this zone are relatively stable, reflecting strong regional market integration, a well-balanced energy mix, and a more predictable supply–demand structure. The key electricity price characteristics analyzed in this study for Scenario 1 are as follows: the mean electricity price is 129.2 €/MWh, with a standard deviation of 127.9 €/MWh. The average daily price differential – a measure of typical daily price fluctuations – is 184.7 €/MWh. The hourly profile in Fig. 2a confirms that Scenario 1 experiences moderate fluctuations around the mean, with a few extreme price spikes throughout the year. The histogram in Fig. 2b (blue color) further supports this stability, showing that most prices are clustered in the lower to mid-price range, with only limited instances of high prices. This dataset was selected as a representative example of a low-volatility market, where prices remain relatively stable with moderate fluctuations.

3.2. Scenario 2: High electricity price variability

Scenario 2 corresponds to the Romanian bidding zone, which represents a highly volatile electricity market within Europe where prices experience frequent and unpredictable variations throughout the year due to dynamic supply–demand conditions. The key electricity price characteristics for Scenario 2 are as follows: the mean electricity price is 265.3 €/MWh, with a standard deviation of 142.9 €/MWh. The average daily price differential in this scenario is 233.5 €/MWh. The higher standard deviation in Scenario 2 reflects increased market volatility, but more importantly, the daily price differential is significantly larger than in Scenario 1, indicating wider price swings within each day. This suggests that electricity prices fluctuate not only over longer periods but also within short time frames, creating an unpredictable market environment. As depicted in Fig. 2a, the hourly profile shows frequent and pronounced price peaks, which reflects substantial price fluctuations over time. Additionally, the histogram in Fig. 2b (orange color) highlights this increased variability, displaying a broader and more dispersed distribution of prices, with frequent occurrences of high prices.

4. Result and discussion

This section presents the results of the technical, economic, and operational analysis of the optimized battery storage system under two distinct market scenarios: Scenario 1 (low-price variability) and Scenario 2 (high-price variability). These results are obtained using proposed operational optimization strategy, which dynamically adjusts cycle characteristics in response to market fluctuations. By analyzing these results, the impact of market price fluctuations on profitability, battery lifespan, overall battery performance, and operational optimization decisions is evaluated. First, the technical and economic performance results are presented (Section 4.1). Next, the influence of each scenario on the battery's SOH over its lifetime is assessed (Section 4.2). Then, the battery SOC dynamics under Scenarios 1 and 2 are examined (Section 4.3). Finally, Section 4.4 provides an in-depth analysis of how the optimization strategy dynamically adjusts key operational parameters to balance revenue generation with battery longevity in response to varying market conditions.

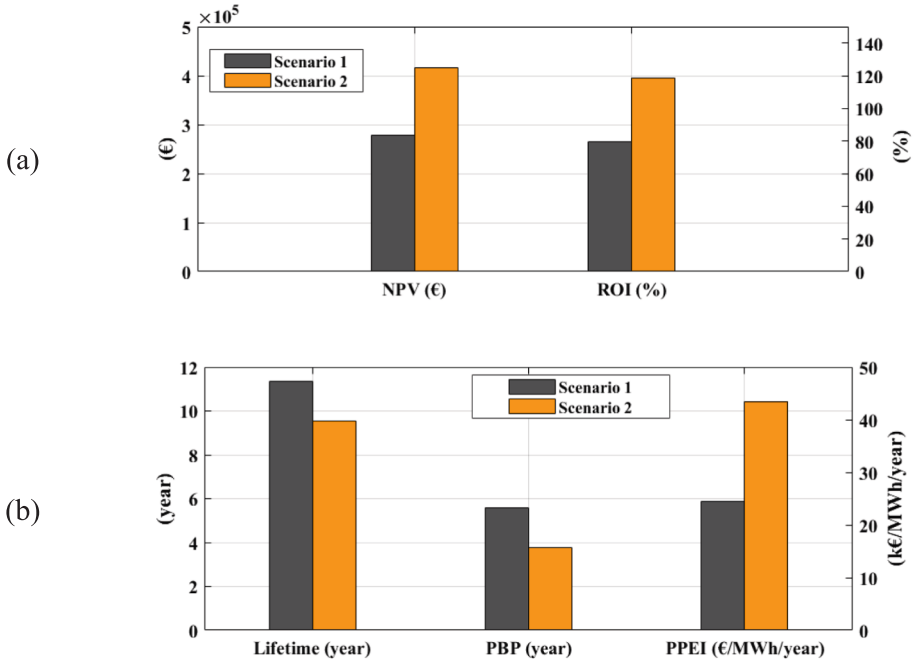

Fig. 3. Comparison of (a) NPV and ROI, (b) battery lifetime, and PBP, and PPEI, under two market scenarios (Scenario 1: low-price variability, and Scenario 2: high-price variability).

4.1. Technical and economic performance results under scenarios 1 and 2

Fig. 3 illustrates a comparative analysis of the financial and technical performance of a 1 MWh grid-connected battery storage system under two market scenarios_Scenario 1 (low-price variability), and Scenario 2 (high-price variability). Table 1 provides the corresponding numerical values for further clarity.

Under Scenario 2 (high-price variability), each 1 MWh installed system generates an average of €43,500 per year, nearly double the €24,500 per year in Scenario 1 (lower-price variability). While PPEI provides insight into short-term profitability, a more comprehensive evaluation of financial viability over the battery's lifetime requires considering additional metrics such as NPV, ROI, and PBP. In Scenario 2, the system achieves an NPV approximately 50 % higher than that in Scenario 1, and an ROI of 118.7 %, versus 79.7 % in Scenario 1. This financial advantage in Scenario 2 stems from frequent price fluctuations, which provide favorable conditions for the operational optimization strategy to capitalize on greater price differentials by charging at low prices and discharging during peaks. In contrast, Scenario 1's stable pricing environment offers fewer such opportunities, yielding relatively lower returns. Another complementary indicator of financial viability is the payback period, which reflects how quickly the initial investment is recovered. In Scenario 2, the payback period is 3.7 years, about 35 % shorter than the 5.6 years in Scenario 1. This faster payback period is due to higher revenue potential from frequent price peaks, making Scenario 2 more attractive from an investment perspective.

The battery in Scenario 1 operates for 11.3 years, whereas in Scenario 2, it lasts for 9.6 years. This difference is due to the adaptable optimization strategy, which adjusts cycle characteristics in response to market conditions and battery state conditions. In Scenario 1, with its stable price environment, the strategy prioritizes battery health, fully leveraging all profitable opportunities while avoiding unnecessary

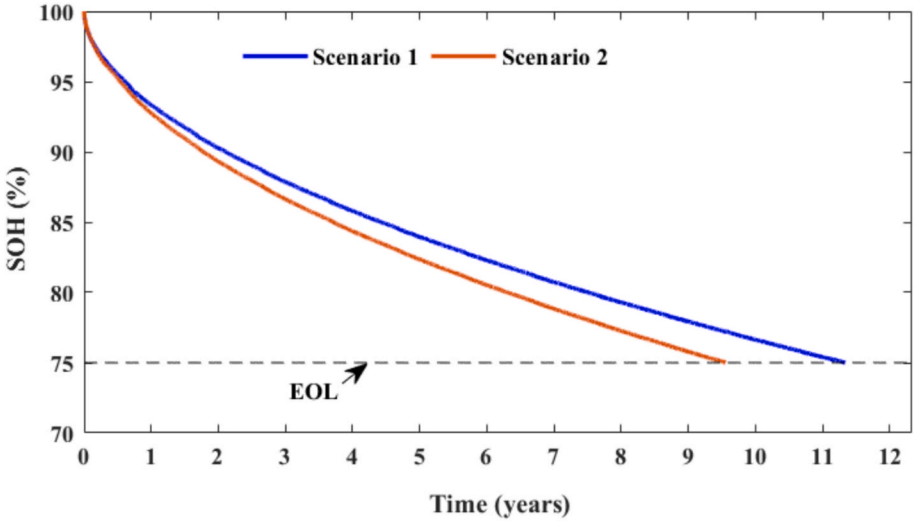

Fig. 4. Time variation of battery SOH over its lifetime under Scenarios 1, and 2.

cycling. In contrast, Scenario 2′s high variability prompts the strategy to intensify cycling to capture frequent price peaks, boosting revenue potential but moderately accelerating degradation. In the following section, it is shown how this adaptability ensures that the strategy dynamically shifts priorities based on market conditions and battery health conditions, optimizing either for extended lifespan or immediate profit depending on the operational environment. The next section explores how these differences affect SOH behavior.

4.2. Battery state-of-health over its lifetime under scenarios 1 and 2

Fig. 4 illustrates the time variation of battery SOH under both market scenarios. The battery is considered to reach the EOL threshold at 75 %, beyond which its operational efficiency declines significantly. In Scenario 1 (low-price variability), the battery's SOH declines at a slower rate, reaching the EOL threshold after approximately 11.3 years. This extended lifespan is attributed to the conservative approach of the optimization strategy under stable market conditions. Under lower price variability scenario, the strategy minimizes cycling frequency and intensity, reducing the stress on the battery, slowing degradation, and extending the battery's useful life. Conversely, in Scenario 2 (high-price variability), the battery reaches the EOL threshold faster, at around 9.3 years. This shorter lifespan results from the optimization strategy's adaptation to frequent price fluctuations in a high-variability market. Here, the strategy intensifies cycling activity to capture rapid, high-value price differentials. Although this accelerates degradation due to more frequent and intense cycles, the increased profitability obtained from cycling outweighs the impact of faster SOH decline. The next section (4.3) provides a detailed analysis of how the optimization strategy dynamically adjusts operational parameters to balance revenue generation and battery longevity.

4.3. Battery state-of-charge dynamics under scenarios 1 and 2

In addition to the SOH evolution, the SOC behavior over the simulation horizon is also examined. To maintain clarity of presentation and avoid excessive complexity, the hourly SOC obtained from simulation and optimization is shown for five representative days rather than for the entire lifetime. Fig. 5 presents the corresponding SOC profiles for Scenarios 1 and 2. As observed, SOC consistently remains within the admissible operating window (10 %–95 %), confirming that the optimization framework effectively enforces the imposed operational constraints over extended horizons. Furthermore, differences between the two scenarios are clearly reflected in the SOC utilization patterns: under the low-volatility scenario, the SOC trajectory exhibits fewer but longer cycles, whereas under the high-volatility scenario, the SOC profile is characterized by more frequent fluctuations, reflecting multiple shorter daily cycles.

4.4. Optimized operational strategies under scenarios 1 and 2

In this section, the adaptive behavior of the optimization strategy is analyzed in response to the distinct market scenarios—Scenario 1 (low-price variability) and Scenario 2 (high-price variability)—focusing on how these conditions affect decisions related to optimal cycle characteristics, including (a) frequency, (b) duration, and (c) start times of charge and discharge cycles. This evaluation reveals how the optimization approach tailors operational parameters to maximize revenue

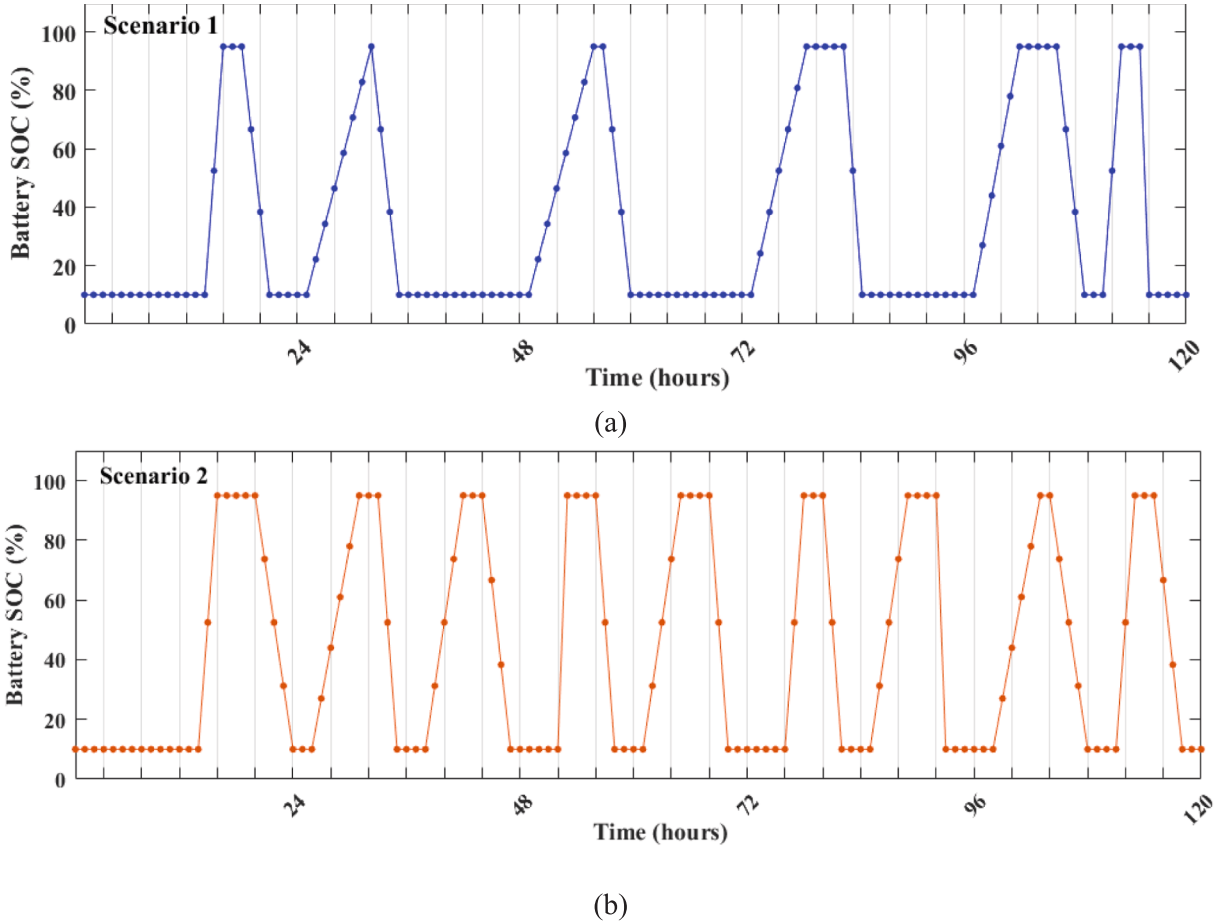

Fig. 5. SOC behavior over five days for (a) Scenario 1 (low volatility) and (b) Scenario 2 (high volatility), illustrating compliance with the admissible SOC range (10%–95%).

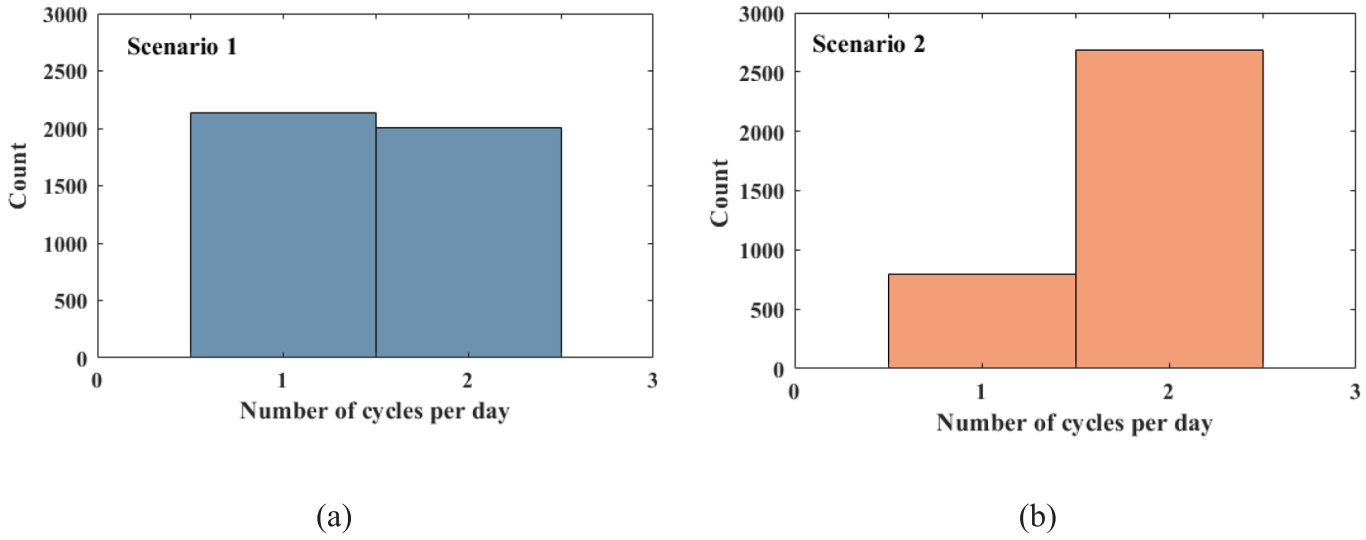

Fig. 6. Comparison of the distribution of the number of cycles per day obtained from the optimization strategy under two market scenarios: (a) Scenario 1 (low price variability), and (b) Scenario 2 (high price variability).

potential while balancing battery degradation across different price variability levels.

4.4.1. Optimal number of cycles per day under scenarios 1 and 2

The cycle frequency distribution shown in Fig. 6 highlights the optimization strategy's responsiveness to different market conditions. In Scenario 1, the battery completes approximately 6,143 cycles over an 11.3-year lifespan, with around 60 % of operational days limited to a single cycle. This conservative approach reduces unnecessary cycling, managing battery degradation and extending lifespan within a stable market. Conversely, in Scenario 2, the battery completes approximately 6,174 cycles over a shorter 9.3-year lifetime, performing two cycles per day on about 80 % of operational days—nearly twice the frequency seen in Scenario 1. This increase is driven by the highly volatile nature of the market, where multiple significant price differentials occur within a single day, providing opportunities for the battery to exploit through more frequent high-value charge–discharge events. The higher cycling frequency in Scenario 2 demonstrates the strategy's adaptability to greater price fluctuations. It should be noted that the second daily cycle in Scenario 2 is not scheduled unconditionally, but only when the marginal revenue outweighs the associated marginal degradation cost. This trade-off is embedded in the optimization objective, which jointly considers revenue and degradation cost. The economic implications of this operational pattern are reflected in the financial analysis presented in Sections 4.1 and 4.2, where Scenario 2 demonstrates substantially higher annual revenue, NPV, and ROI, and a shorter payback period, despite a moderately reduced lifetime. These results confirm that the additional cycling observed in Scenario 2 remains economically justified.

4.4.2. Charge and discharge duration under scenarios 1 and 2

The charge and discharge durations represent two critical decision variables in the proposed optimization strategy, adapting to market dynamics and exhibiting distinct patterns under the two scenarios, as illustrated in Figs. 7 and 8. The distribution of optimal charge durations between Scenario 1 and Scenario 2 (Fig. 7) highlights the clear differences. Under Scenario 1 (low-price variability), around 60 % of the charge durations fall within the 4–10 h range, with the remaining durations spread across shorter intervals (1–3 h), reflecting a preference for longer charge durations (i.e., slower C-rates). Conversely, in Scenario 2 (high-price variability), around 80 % of charge durations are concentrated within the shorter 1–3 h range, with about 40 % specifically clustered at 2 h, indicating a significantly faster charging approach. The frequency of these shorter durations in Scenario 2 is nearly double that

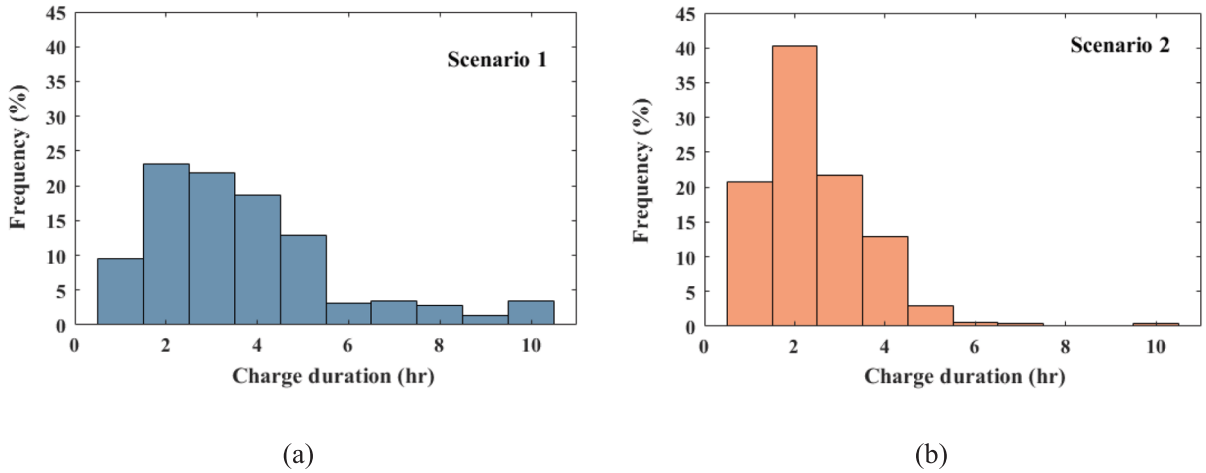

Fig. 7. Comparison of histograms of optimized charge durations over battery lifetime obtained from the optimization strategy under two market scenarios: (a) Scenario 1 (low price variability), and (b) Scenario 2 (high price variability).

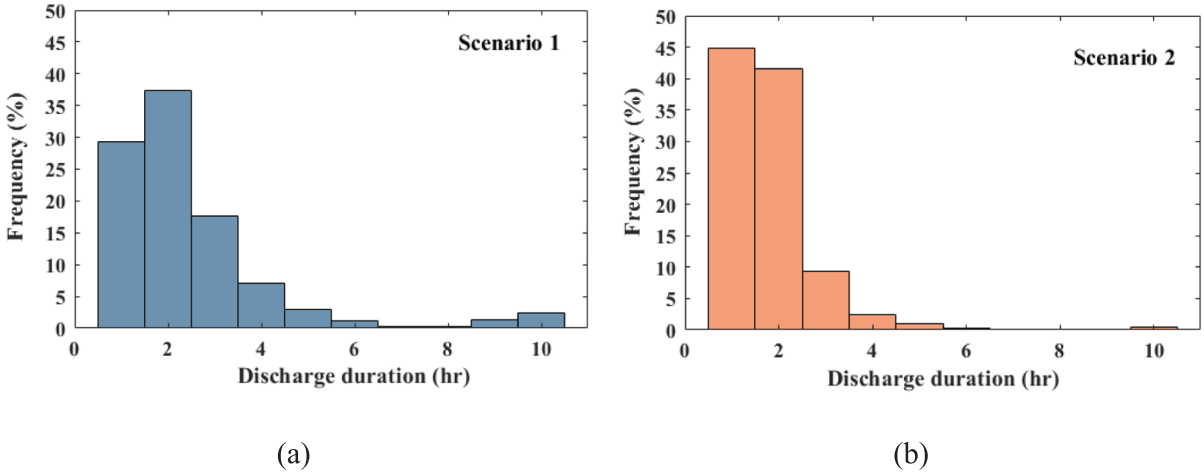

Fig. 8. Comparison of optimized discharge durations over battery lifetime obtained from the optimization strategy under two market scenarios: (a) Scenario 1 (low price variability), and (b) Scenario 2 (high price variability).

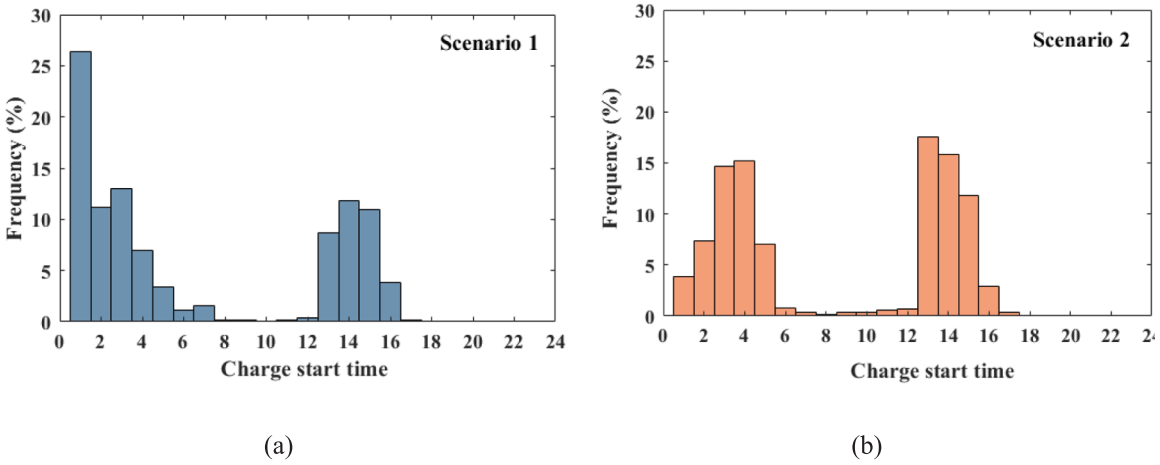

Fig. 9. Comparison of histogram of optimized charge start times over battery lifetime obtained from optimization strategy under two market scenarios (a) Scenario 1 (low-level price variability) (b) Scenario 2 (high-level price variability).

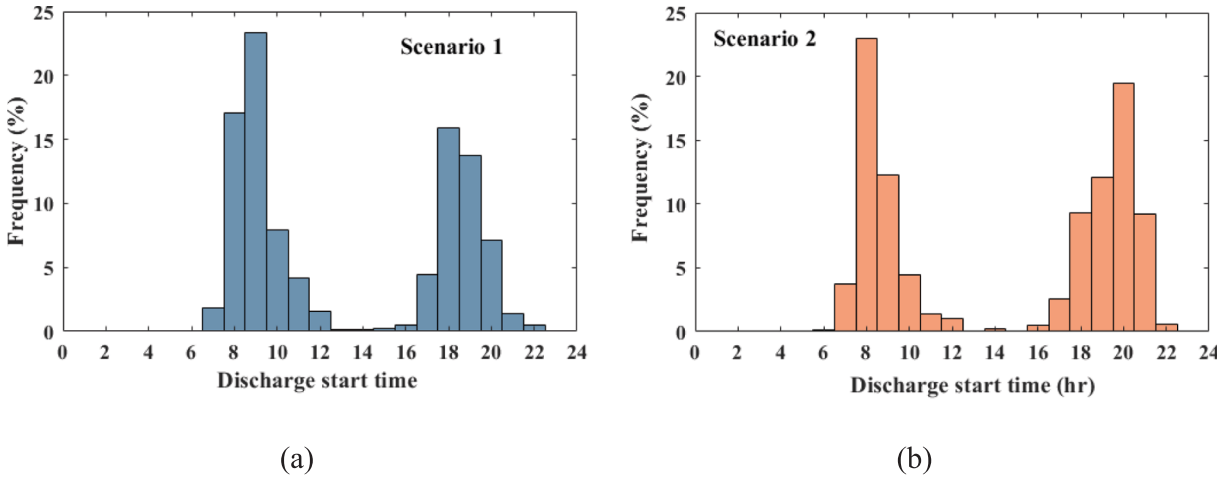

Fig. 10. Comparison of optimized discharge start times over battery lifetime obtained from optimization strategy under two market scenarios (a) Scenario 1 (low-level price variability) (b) Scenario 2 (high-level price variability).

of Scenario 1.

Similarly, the distribution of optimal discharge durations shows distinct differences under the two scenarios (Fig. 8). In Scenario 1, approximately 60 % of discharge durations fall within the 1–2 h range, while the remaining 40 % are distributed across longer durations. By contrast, in Scenario 2, approximately 90 % of discharge durations are concentrated within the shorter 1–2 h range, with a notable peak of about 45 % at just 1 h.

The broader and longer-duration approach observed in Scenario 1 reflects a conservative strategy aimed at prioritizing battery longevity. Given the stable price environment in Scenario 1, there are fewer high-value opportunities requiring rapid cycling, enabling the optimization strategy to reduce cycle intensity and limit degradation. In contrast, Scenario 2 exhibits shorter and more compressed charge and discharge durations, representing an aggressive, profit-driven approach. Frequent price fluctuations under high-price variability offer numerous revenue opportunities, thus, shorter charge and discharge durations (higher rates) enable the battery to rapidly respond to price spikes, increasing immediate profitability. Although this higher cycling intensity could accelerate degradation, the optimization strategy dynamically balances this trade-off by selecting operational parameters only when the financial gains exceed the associated degradation costs.

4.4.3. Charge and discharge start times under scenarios 1 and 2

As illustrated in Figs. 9 and 10, charge and discharge start times adapt distinctly to market dynamics under each scenario. As shown in Fig. 9(a), under Scenario 1 (low-price variability), approximately 65 % of charging events occur in the early morning (1–7 AM), with 56 % specifically between 1 and 4 AM. Additionally, another off-peak window for charging arises in the early afternoon (12–4 PM), with around 22 % of charging events starting between 2 and 3 PM. This pattern allows the battery to effectively exploit midday off-peak prices. In contrast, under Scenario 2 (high-price variability), about 50 % of charging events occur in the early morning (1–6 AM), with a higher concentration (45 %) between 2 and 5 AM. The remaining 50 % of charge start times are spread between 10 AM and 5 PM, peaking around 1–3 PM (46 %), indicating increased utilization of secondary off-peak opportunities to capitalize on multiple daily periods of lower prices.

Similarly, discharge start times reflect the market conditions of each scenario, as depicted in Fig. 10. In Scenario 1, approximately 60 % of discharge events are concentrated between 7 and 12 AM, with the majority (40 %) occurring around 8–9 AM, aligning with morning price peaks. Additionally, another discharge events (about 35 %) occurs between 4 and 10 PM, peaking around 6–8 PM. In Scenario 2, around 45 % of discharges are initiated between 7 AM and 12 PM, while the remaining discharges are distributed between 3 PM and 10 PM, with a peak concentration (around 50 %) between 6 and 9 PM. This increased utilization of a second discharge peak provides additional opportunities for the battery to maximize revenue by strategically responding to more frequent and pronounced price peaks in the highly volatile market environment.

5. Conclusion

This study demonstrates that the proposed condition-responsive optimization strategy effectively adjusts battery charge–discharge behavior in response to electricity market dynamics, striking a balance between revenue generation and battery longevity. The framework exhibited strong adaptability across the studied market conditions: in low-price variability scenarios, it adopted a conservative approach—favoring battery health by limiting cycling frequency and extending charge–discharge durations. Conversely, in high-price variability environments, the strategy shifted to a more aggressive, profit-driven mode, enabling the battery to capitalize on multiple daily price spikes through shorter, more frequent cycles.

The study confirms that adaptive strategies can substantially enhance the financial performance of battery storage compared to conventional static or rule-based scheduling approaches. Although high market volatility accelerates degradation, the proposed strategy ensures that additional cycling is economically justified, yielding higher returns while maintaining nearly a decade of operational life.

Overall, the findings highlight the importance of embedding market-aware, adaptive scheduling into energy storage operation frameworks. The study provides practical insights for system operators, investors, and policymakers on tailoring storage strategies to different price environments, thereby supporting the development of more profitable, resilient, and sustainable energy systems.

CRediT authorship contribution statement

Masoume Shabani: Writing – review & editing, Writing – original draft, Visualization, Validation, Supervision, Software, Resources, Methodology, Investigation, Formal analysis, Data curation, Conceptualization.

Declaration of competing interest

The author declares that they have no known competing financial interests or personal relationships that could have appeared to influence the work reported in this paper.

Acknowledgment

The author would like to thank Prof. Jinyue Yan for his academic guidance and support. The author also thanks Mohadeseh Shabani and Prof. Daniel Brandell for reading the final draft.

Appendix A

The terminal voltage during charging and discharging is calculated based on the operating conditions using the relationships defined in Eqs. (A1) and (A2). The state-dependent OCV and R curves are characterized using experimental data and implemented as lookup tables within the simulation framework. For additional technical specifications, modeling and validation details, refer to [52].

$$V_{\mathrm{ch},t}(SOC_t, T, I_t) = OCV_{\mathrm{ch}}(SOC_t, T, I_t) + I_{\mathrm{ch},t} \times R_{\mathrm{ch}}(SOC_t, T, I_t) \tag{A1}$$

$$V_{\mathrm{dch},t}(SOC_t, T, I_t) = OCV_{\mathrm{dch}}(SOC_t, T, I_t) + I_{\mathrm{dch},t} \times R_{\mathrm{dch}}(SOC_t, T, I_t) \tag{A2}$$

At each time step, total capacity-fade is computed using Eq. (A5), which combines contributions from both calendar aging (Eq. (A3)) and cyclic aging (Eq. (A4)). The parameter values used in the model (α_1, α_2, α_3, α_4, α_5, α_6) are listed in Table A1 and the FEC formulation is given in Eq.(A6). Detailed derivations outlining the application of both degradation models (cyclic and calendric) under variable operational conditions can be found in previous work [33].

$$C_{\text{fade, cal}_t}(SOC, time) = \left(\alpha_1 (SOC - 0.5)^3 + \alpha_2\right) \times time^{0.5} \quad \text{(A3)}$$

$$C_{\text{fade, cyc}_t}(C_{rate}, DOC, FEC) = (\alpha_3 . C_{rate} + \alpha_4) \times \left(\alpha_5 (DOC - 0.6)^3 + \alpha_6\right) \times (FEC)^{0.5} \quad \text{(A4)}$$

$$C_{\text{fade, tot}_t}(SOC, time, C_{\text{rate}}, DOC, FEC) = (C_{\text{fade, cal}_t}(SOC, time) + C_{\text{fade, cyc}_t}(C_{\text{rate}}, DOC, FEC)) \times C_{\text{batt, BOL}} \quad \text{(A5)}$$

Table A1
Battery aging parameters [38,40].

	α_1	α_2	α_3	α_4	α_5	α_6
Value	2.8575	0.60225	0.0630	0.0971	4.0253	1.0923

As shown in Eq. (A6), the FEC quantifies the total number of complete charge–discharge cycles that a battery has experienced over time. It is determined by dividing the cumulative charge throughput by twice the battery's rated capacity at the BOL.

$$FEC = \frac{C_{\text{batt, cum}}}{2 \times C_{\text{batt, BOL}}} = \frac{C_{\text{batt, cum, ch}} + C_{\text{batt, cum, dch}}}{2 \times C_{\text{batt, BOL}}} \quad \text{(A6)}$$

Appendix B

Table A2
Characteristics of the studied LFP battery.

Indicator	Value
Battery type	LFP/C
Battery capacity (MWh)	1 MWh
Battery usable capacity	0.85 MWh
Battery maintenance cost (% of investment/year)	0.5 %
Battery energy specific price (€/kWh)	350
Minimum SOC (%)	10 %
Maximum SOC (%)	95 %
Battery lifetime (LF)	Lifetime Model

Appendix C

Derivation of objective function:

$$Revenue_m = \sum_{t=1}^{24} \left(\left(P_{\text{dch},t} \times El_{W,t}\right) - \left(P_{ch,t} \times El_{\text{w},t}\right) \right)_m \quad \text{(C2)}$$

$$Cost_{\text{deg,batt}_m} = \frac{C_{\text{fade, tot}_m}}{1 - \alpha_{\text{Replace}}} \times ICC_{\text{batt}} \quad \text{(C3)}$$

Although Eq. (C3) expresses degradation cost in terms of total capacity fade and unit battery price, the underlying degradation model is nonlinear, as it accounts for dynamic operating conditions such as SOC, DOC, C-rate, and SOH (see Eqs. (A3)-(A5)). Thus, degradation costs are not assumed to increase linearly with time or usage, but are instead dynamically linked to operational stress factors. Eq. (C3) therefore serves as a monetary mapping, converting the operation-dependent nonlinear degradation into cost by applying the unit battery price. It should be noted, however, that the potential residual or second-life value of batteries at EOL is not included in the present formulation, as the focus of this study is on the first life of the battery. A threshold SOH of 75 % is used to define the EOL, consistent with typical warranty specifications for LFP batteries in stationary applications.

Data availability

The authors do not have permission to share data.

References

[1] Maier R, Behrens J, Hoffmann M, Kullmann F, Weinand JM, Stolten D. Impact of foresight horizons on energy system decarbonization pathways. Adv Appl Energy 2025 Jun;1(18):100217.
[2] IRENA 2024. Renewable Energy Highlights. https://www.irena.org/-/media/Files/IRENA/Agency/Publication/2024/Jul/Renewable_energy_highlights_FINAL_July_2024.pdf (accessed Dec, 2024).
[3] Ruggles TH, Virgüez E, Reich N, Dowling J, Bloomfield H, Antonini EG, et al. Planning reliable wind-and solar-based electricity systems. Adv Appl Energy 2024 Sep;1(15):100185.
[4] Hu J, Koning V, Bosshard T, Harmsen R, Crijns-Graus W, Worrell E, et al. Implications of a Paris-proof scenario for future supply of weather-dependent variable renewable energy in Europe. Adv Appl Energy 2023 Jun;1(10):100134.
[5] Mlilo N, Brown J, Ahfock T. Impact of intermittent renewable energy generation penetration on the power system networks–a review. Technol Econ Smart Grids Sustain Energy 2021 Dec 10;6(1):25.
[6] Navia Simon D, Diaz AL. Power price stability and the insurance value of renewable technologies. Nat Energy 2025 Jan;28:1–3.
[7] Batalla-Bejerano J, Trujillo-Baute E. Impacts of intermittent renewable generation on electricity system costs. Energy Policy 2016 Jul;1(94):411–20.

[8] Brouwer AS, Van Den Broek M, Seebregts A, Faaij A. Impacts of large-scale intermittent renewable energy sources on electricity systems, and how these can be modeled. Renew Sustain Energy Rev 2014 May;1(33):443–66.
[9] Göransson L. Balancing electricity supply and demand in a carbon-neutral Northern Europe. Energies. 2023;16(8):3548.
[10] Chatzigeorgiou NG, Theocharides S, Makrides G, Georghiou GE. A review on battery energy storage systems: applications, developments, and research trends of hybrid installations in the end-user sector. J Energy Storage 2024;86:111192.
[11] IEA. Grid-scale storage https://www.iea.org/energy-system/electricity/grid-scale-storage (accessed Nov, 2024).
[12] Shabani M, Shabani M, Wallin F, Dahlquist E, Yan J. Smart and optimization-based operation scheduling strategies for maximizing battery profitability and longevity in grid-connected application. Energy Convers Manage: X 2024 Jan;1(21):100519.
[13] Su H, Feng D, Zhou Y, Hao X, Yi Y, Li K. Impact of uncertainty on optimal battery operation for price arbitrage and peak shaving: from perspectives of analytical solutions and examples. J Energy Storage 2023 Jun;1(62):106909.
[14] Fridgen G, Kahlen M, Ketter W, Rieger A, Thimmel M. One rate does not fit all: an empirical analysis of electricity tariffs for residential microgrids. Appl Energy 2018 Jan;15(210):800–14.
[15] Hu Z, Kim JH, Wang J, Byrne J. Review of dynamic pricing programs in the US and Europe: status quo and policy recommendations. Renew Sustain Energy Rev 2015 Feb;1(42):743–51.
[16] Núñez F, Canca D, Arcos-Vargas´A. An assessment of European electricity arbitrage using storage systems. Energy 2022;242:122916.
[17] Bradbury K, Pratson L, Patíño-Echeverri D. Economic viability of energy storage systems based on price arbitrage potential in Mustafa. Appl Energy 2014;114:512–9.
[18] Metz D, Saraiva JT. Use of battery storage systems for price arbitrage operations in the 15-and 60-min German intraday markets. Electric Pow Syst Res 2018 Jul;1(160):27–36.
[19] Campana PE, Cioccolanti L, François B, Jurasz J, Zhang Y, Varini M, et al. Li-ion batteries for peak shaving, price arbitrage, and photovoltaic self-consumption in commercial buildings: a Monte Carlo Analysis. Energy Convers Manag 2021;234:113889.
[20] Komorowska A, Olczak P, Hanc E, Kamíński J. An analysis of the competitiveness of hydrogen storage and Li-ion batteries based on price arbitrage in the day-ahead market. Int J Hydrogen Energy 2022 Aug 1;47(66):28556-72.
[21] Shcherbakova A, Kleit A, Cho J. The value of energy storage in South Korea's electricity market: a hotelling approach. Appl Energy 2014 Jul;15(125):93–102.
[22] Lin B, Wu W. Economic viability of battery energy storage and grid strategy: a special case of China electricity market. Energy 2017;124:423–34.
[23] Peñaranda AF, Romero-Quete D, Cortés CA. Grid-scale battery energy storage for arbitrage purposes: a Colombian case. Batteries 2021 Sep 3;7(3):59.
[24] Dufo-López R. Optimisation of size and control of grid-connected storage under real time electricity pricing conditions. Appl Energy 2015 Feb;15(140):395–408.
[25] Berg K, Resch M, Weniger T, Simonsen S. Economic evaluation of operation strategies for battery systems in football stadiums: a Norwegian case study. J Energy Storage Feb. 2021;34:102190.
[26] Mustafa MB, Keatley P, Huang Y, Agbonaye O, Ademulegun OO, Hewitt N. Evaluation of a battery energy storage system in hospitals for arbitrage and ancillary services. J Energy Storage 2021 Nov;1(43):103183.
[27] Komorowska A, Olczak P. Economic viability of Li-ion batteries based on the price arbitrage in the European day-ahead markets. Energy 2024 Mar;1(290):130009.
[28] Telaretti E, Ippolito M, Dusonchet L. A simple operating strategy of small-scale battery energy storages for energy arbitrage under dynamic pricing tariffs. Energies 2015 Dec 25;9(1):12.
[29] Shabani M, Wallin F, Dahlquist E, Yan J. The impact of battery operating management strategies on life cycle cost assessment in real power market for a grid-connected residential battery application. Energy 2023 May;1(270):126829.
[30] Telaretti E, Sanseverino ER, Ippolito M, Favuzza S, Zizzo G. A novel operating strategy for customer-side energy storages in presence of dynamic electricity prices. Intel Ind Syst 2015 Oct;1:233–44.
[31] Mohsenian-Rad H. Optimal bidding, scheduling, and deployment of battery systems in California day-ahead energy market. IEEE Trans Power Syst 2016;31(1):442–53.
[32] Wankmüller F, Thimmapuram PR, Gallagher KG, Botterud A. Impact of battery degradation on energy arbitrage revenue of grid-level energy storage. J Energy Storage 2017 Apr;1(10):56–66.
[33] Shabani M, Wallin F, Dahlquist E, Yan J. Techno-economic assessment of battery storage integrated into a grid-connected and solar-powered residential building under different battery ageing models. Appl Energy 2022 Jul;15(318):119166.
[34] Gao Y, Jiang J, Zhang C, Zhang W, Ma Z, Jiang Y. Lithium-ion battery aging mechanisms and life model under different charging stresses. J Power Sources 2017 Jul;15(356):103–14.
[35] Stroe DI. Lifetime models for Lithium-ion batteries used in virtual power plant applications. Ph.D. dissertation. Aalborg, Denmark: Dept. of Energy Tech., Aalborg University; 2014.
[36] Naumann M, Schimpe M, Keil P, Hesse HC, Jossen A. Analysis and modeling of calendar aging of a commercial LiFePO4/graphite cell. J Storage 2018 Jun;1(17):153–69.
[37] Teliz E, Zinola CF, Díaz V. Identification and quantification of ageing mechanisms in Li-ion batteries by Electrochemical impedance spectroscopy. Electrochim Acta 2022 Sep;10(426):140801.
[38] Naumann M, Spingler FB, Jossen A. Analysis and modeling of cycle aging of a commercial LiFePO4/graphite cell. J Power Sources 2020 Mar;1(451):227666.
[39] Šeruga D, Gosar A, Sweeney CA, Jaguemont J, Van Mierlo J, Nagode M. Continuous modelling of cyclic ageing for lithium-ion batteries. Energy 2021 Jan;15(215):119079.
[40] Terlouw T, AlSkaif T, Bauer C, van Sark W. Multi-objective optimization of energy arbitrage in community energy storage systems using different battery technologies. Appl Energy Apr. 2019;239:356–72.
[41] Lujano-Rojas JM, Dufo-López R, Bernal-Agustín JL, Catalão JP. Optimizing daily operation of battery energy storage systems under real-time pricing schemes. IEEE Trans Smart Grid 2016 Aug 24;8(1):316–30.
[42] Ahlert KH, Van Dinther C. Sensitivity analysis of the economic benefits from electricity storage at the end consumer level. In: 2009 IEEE Bucharest PowerTech 2009 Jun 28 (pp. 1-8). IEEE.
[43] Sioshansi R, Denholm P, Jenkin T, Weiss J. Estimating the value of electricity storage in PJM: arbitrage and some welfare effects. Energy Econ 2009;31(2):269–77.
[44] Walawalkar R, Apt J, Macini R. Economics of electric energy storage for energy arbitrage and regulation in New York. Energy Policy 2007;35:2258–568.
[45] Li Y, Vilathgamuwa M, Farrell TW, Tran NT, Teague J. Development of a degradation-conscious physics-based lithium-ion battery model for use in power system planning studies. Appl Energy 2019 Aug;15(248):512–25.
[46] Xu B, Zhao J, Zheng T, Litvinov E, Kirschen DS. Factoring the cycle aging cost of batteries participating in electricity markets. IEEE Trans Power Syst 2018;33(2):2248–59.
[47] Kazemi M, Zareipour H. Long-term scheduling of battery storage systems in energy and regulation markets considering battery's lifespan. IEEE Trans Smart Grid 2018;9(6):6840–9.
[48] Tan X, Wu Y, Tsang DHK. A stochastic shortest path framework for quantifying the value and lifetime of battery energy storage under dynamic pricing. IEEE Trans Smart Grid 2017;8(2):769–78.
[50] Hesse HC, Schimpe M, Kucevic D, Jossen A. Lithium-ion battery storage for the grid—a review of stationary battery storage system design tailored for applications in modern power grids. Energies 2017 Dec;10(12):2107.
[51] Katrašnik T, Mele I, Zelič K. Multi-scale modelling of Lithium-ion batteries: from transport phenomena to the outbreak of thermal runaway. Energy Convers Manage 2021 May;15(236):114036.
[52] Shabani M, Dahlquist E, Wallin F, Yan J. Techno-economic impacts of battery performance models and control strategies on optimal design of a grid-connected PV system. Energy Convers Manage 2021 Oct;1(245):114617.
[53] Chang WY. The state of charge estimating methods for battery: a review. Int Scholar Res Not 2013;2013(1):953792.
[54] Lei X, Zhong J, Chen Y, Shao Z, Jian L. Grid Integration of Electric Vehicles within Electricity and Carbon Markets: A Comprehensive Overview. eTransportation. 2025 Jun 6:100435.
[55] Lei X, Yu H, Yu B, Shao Z, Jian L. Bridging electricity market and carbon emission market through electric vehicles: optimal bidding strategy for distribution system operators to explore economic feasibility in China's low-carbon transitions. Sustain Cities Soc 2023 Jul;1(94):104557.
[56] ENTSO-E Day-ahead electricity prices < https://www.entsoe.eu/data/ > [accessed 1 Dec. 2024].